



ISSN: 2454-9940



**INTERNATIONAL JOURNAL OF APPLIED
SCIENCE ENGINEERING AND MANAGEMENT**

E-Mail :
editor.ijasem@gmail.com
editor@ijasem.org

www.ijasem.org

OPTIMIZING VOLTAGE STABILITY: LEVERAGING INTEGRATED PHOTOVOLTAIC SYSTEM AND DYNAMIC VOLTAGE RESTORER

#1 Mr. MATHANGI SRIKANTH, *Asst. Professor*,

#2 Mr. PURELLA SRAVAN KUMAR, *Asst. Professor*,

Department of Electrical and Electronics Engineering,

Sree Chaitanya Institute Of Technological Sciences, Karimnagar, Ts.

ABSTRACT: With the increased penetration of sensitive loads, distribution energy satisfaction challenges have grown, particularly in renewable energy resources. A novel technique for integrating a grid-connected photovoltaic system with a self-supported dynamic voltage restorer (DVR). Its primary function is to inject active power into the PV array via MPPT control and to maintain constant load terminal voltage, with DVR being the most practical alternative. The term "six-port converter" refers to all nine semiconductor switches in this proposed technology. This setup allows the utility grid and the six-port converter to exchange energy in both directions. On all operational modes, a manipulation algorithm and a learn are built. Extensive modeling and experimental reports under extreme operating conditions back up the proposed arrangement. The MATLAB-focused history allows you to design this new DVR configuration with PV more quickly and precisely.

Index Terms: Bidirectional power flow, Distributed power generation, Photovoltaic (PV) systems, Power quality, Voltage control.

1. INTRODUCTION

Due to the increasing depletion of conventional energy sources and growing environmental concerns, photovoltaic (PV) and wind energy are new sources of electricity. Grid-linked PV requires a dc-ac inversion stage because its energy is mostly dc. A three-section voltage source inverter (VSI) with six switches is normally the core of a grid-connected photovoltaic system. As sensitive populations become more widespread, advanced distribution system energy efficiency challenges have increased. High-vigor point tracking (MPPT) PV array control boosts injected energetic vigor. Faults, swells, and sags produce most grid voltage disturbances.

Several power devices are used to maintain load terminal voltage, but DVR is the best and most complete option.

Modern load facilities may have custom vigor devices and online PV fresh release units for load security. This shows that a self-supported DVR employs a second six-swap VSI (DVR-VSI) to adjust for voltage sag for sensitive masses, while a grid-related PV plant injects active energy. The fault/deep sag event at the point of fashioned coupling (PCC) limits these objective PV and DVR techniques. The self-supported DVR cannot maintain the rated load voltage due to the dc-link capacitor's limited energy. Photovoltaic electricity cannot be sold to the grid. A

load-side shunt rectifier can charge the dc-hyperlink capacitor at rated price for DVR. However, the DVR-VSI setup must be rated for each load and shunt rectifier VA due to massive VA loading. Replace the DC-hyperlink capacitor with a battery power storage solution to boost DVR performance. It doesn't affect DVR rating, but it does compromise battery life.

The VA rating of the centralized PV inverter depends on the PV sun panels' setup. Sunshine energy is intermittent, hence this inverter VA is rarely used. During late evening, early morning, and nights, it is inactive. However, DVR VA scores account for 20%–40% of VA loading. Due to the voltage disturbance being temporary and energy-efficient, the DVR inverter has a low-utilization element. The multi loop control technique dampens DVR LC harmonic filter resonant oscillations and provides steady-state performance and transient responsiveness. This work proposes a six-port converter-based system architecture, shown in Fig., to combine an on-site PV generation unit with DVR. 2. The suggested architecture solves the operating limits of standard PV and DVR systems, most importantly. The conventional system has 25% fewer switches since it eliminates the requirement for two PV and DVR inverters. If onsite PV generation capacity exceeds 50% of load need, the suggested setup may benefit manufacturers or low- to medium-power load centers with sensitive loads. The six-port converter's VA rating will depend on the PV system's VA rating. This means that DVR regulates load voltage like the PV system.

The literature suggests using the six-port converter instead of back-to-back converters in micro grids, rectifier-inverter

systems, uninterrupted power supply (UPQC), and twin motor drives. Recent reports described improving fault ride through of DFIG-based wind energy conversion system using nine switch-based converters. The suggested layout of Fig. 2 retains the major components of the standard 12-switch arrangement in Fig. 1. It replaces two distinct VSIs with one integrated converter and reduces semiconductors, gate drive, and control circuitry by 25%. The configuration allows bidirectional active power flow between the utility grid, PV plant, and six-port converter, which smooths sag adjustment to protect delicate loads during acute PCC voltage dips. Simulations are used to evaluate the proposed work before experiments are conducted.

2.PROPOSED CONFIGURATION AND CONTROL STRATEGY PROPOSED INTEGRATED PV-DVR SYSTEM

Fig. displays recommended system settings. 2. This arrangement uses nine semiconductor switches for PV and DVR simultaneous operation. This system differs most from Fig. and suggested setup. Two sets of outputs are on a dual output six-port converter. PV-VSI outputs indicate left three ports (a, b, c) connected to PCC, while DVR-VSI outputs are right three ports (x, y, z). DVR and PV VSIs share S4–S6 switches. The six-port converter can operate in any of Table I's modes depending on the PV plant and grid.

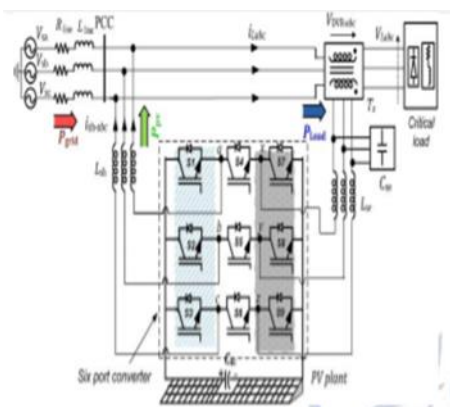


Fig 1:

Recommended PV-DVR setup.

Interleaving Technique with Different OPERATING MODES Action of DVR:

The main function of a DVR is to protect sensitive loads from network power surges. The DVR is near fragile loads. The DVR inserts the series voltage VDVR and adjusts the load voltage to the pre-failure value if other lines fail. The three injected phase voltages' momentary amplitudes are adjusted to prevent bus faults from affecting load voltage VL. This means that any differential voltages caused by brief ac feeder disturbances will be countered by a converter-produced voltage, which will be injected via the booster transformer at medium voltage. No matter the problem or occurrence, the DVR will work if the system stays connected to the supply grid and the line breaker doesn't trip. Balancing the positive and negative sequence components of the voltage disturbance at the DVR's input usually yields a cheaper design. This option is fair because the step down transformer's infinite impedance prevents the zero sequence component of a disturbance from passing through it in a regular distribution bus.

The DVR has boost and standby modes. The converter shorts the booster transformer's low voltage winding in standby mode (VDVR=0). Each converter

leg is activated to provide a transformer short circuit path, so no semiconductors are switched. Therefore, only the semiconductors' low conduction losses create losses in this current loop. Usually, the DVR is in this mode. In boost mode (VDVR>0), the DVR detects supply voltage disturbances and injects a compensatory voltage through the booster transformer.

HEALTHY MODE:

Mode-1 shows the six-port converter's normal behavior when the grid voltage is nominal and the PV facility is operating under SAC. PV-VSI injects PV plant power into the grid in Mode 1 while DVR-VSI is inactive due to grid stability. Figure. Figure 3 shows the six-port converter's comparable operational circuit and switch conditions. Carrier-based modulation generates each switch's gating signal pattern (see Section III). See Fig. In Mode-1, switches S7-S9 in Table I and Figure 3 are always "ON" (logical high), while switches S1-S6 are in the pulse width modulation (PWM) control state, enabling PV-VSI. When S7 through S9 are ON, the series injection transformer's primary windings are shorted out, preventing DVR-VSI from supplying active power.

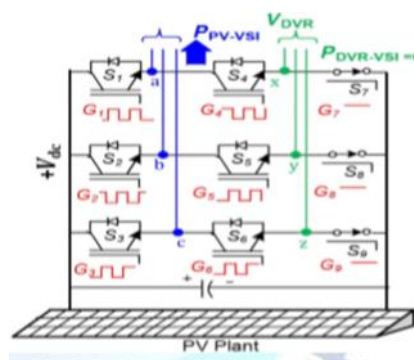


Fig.2: Equivalent Circuit Representation.

FAULT MODE

Mode-2 is a three-phase PCC fault. In this

mode, DVR-VSI injects the greatest compensating voltages while PV-VSI sleeps. PV supports critical load as a DVR through switches S4–S9. Unconnected to the utility grid. The suggested configuration's Mode-2 feature cannot be implemented in Fig. due to the typical PV and self-supported DVR system failing during a three-phase PCC breakdown. 1. S1–S3 are always ON because the PV-VSI coupling inductor provides the series transformer's neutral point. There may be a voltage drop across these inductors, but the DVR can readily compensate.

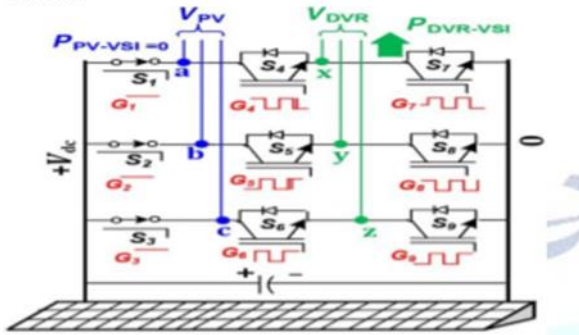


Fig.3: Incorrect Mode

SAGMODE

Mode-3 considers how the six-port converter at PCC reacts to voltage drops. In VLabc mode, the DVR-VSI does pre-sag compensation to avoid the critical load from tripping too soon. The three leftmost switches of the six have gating signals due to large phase leaps. Non-zero grid voltage keeps the port converter at logic high. In Mode-2, switches S1 through S3 are always ON (see Fig.). 4. As shown in 2.6, the PV plant running at SAC activates DVR and PV-VSI (all nine switches) during Mode-3. The PV plant receives restricted active power from the six-port converter based on maximum current capacity.

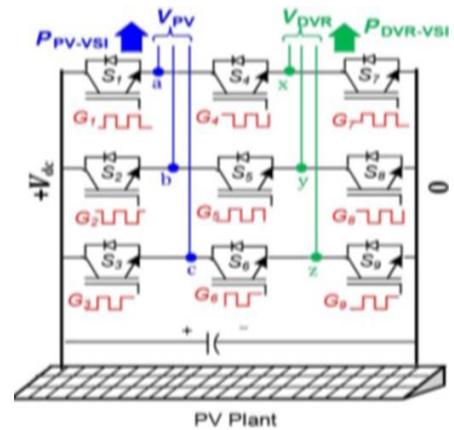


Fig.:4: Dim Mode

NO PV GENERATION

When the PV plant is dormant, it functions in Mode 4, like a six-port converter. These include early morning, late evening, cloudy days, and all night. PV-VSI works oppositely without a PV plant. The dc-link capacitor gets active power from the grid during sag intervals and is idle while the grid is at its rated voltage to keep it charged. The mode's depiction resembles Mode-3 (Fig.). 6 except for inverted PV-VSI active power flow (grid-to-dc link). When the current need exceeds the switch current rating, severe or deeper sag depths prevent dc-link regulation. This equation determines the capacitor size Cdc.

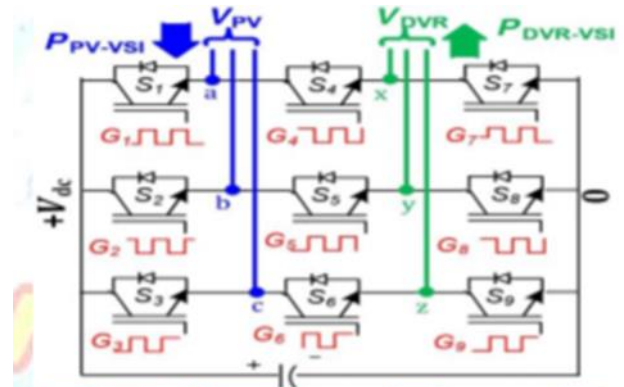


Fig.5

Comparable System

Different Modes of Operation:

Mode	PV status	Grid condition	Switch status		Six-port converter operation	
			Always 'on'	PWM	PV-VSI	DVR-VSI
1	Active	Healthy $V_{30-90} = 1$	S ₁ -S ₃	S ₄ -S ₆	Active ($P_{PV} > 0$)	Idle ($P_{DVR} = 0$)
2	Active	Fault $V_{30-90} = 0$	S ₁ -S ₃	S ₄ -S ₆	Idle ($P_{PV} = 0$)	Active ($P_{DVR} = P_{Load}$)
3	Active	Sag $1 < V_{30-90} < 0.95$	None	S ₁ -S ₃	Active ($P_{PV} > 0$)	Active ($P_{DVR} < P_{Load}$)
4	Inactive	Any of the above 3	None	S ₁ -S ₃	Active ($P_{PV} < 0$)	Active

3. MODULATION SCHEME FOR PROPOSED CONVERTER

Switching modes

See Fig. 2. Three switches on the six-port converter serve PV and DVR-VSIs. The allowed switching states are limited. Two output ports on the same leg have four connectivity options. Phase-a: S1-ON, S4-ON, and S7-OFF; 1) both outputs to +Vdc; 2) both to 0 V (Polisetty Hema Sundar: Dynamic Voltage Restorer with Integrated Photovoltaic System to reduce voltage fluctuations in faulty conditions."

Phase-a: S1 ON, S4 ON, S7 ON; 3) left port to +Vdc, right port to 0 V S1-ON, S4-ON, and S7-ON); and 4) set left port to 0 V and right port to +Vdc (phase-a).

Comparison of signal

Due to direct DC link short circuiting, the last combination is impossible. Modulation and gate pulses are generated by comparing both reference signals to a common carrier. Using a common carrier

Third harmonic injection raises the left port's modulation reference signal above the right's without affecting the six-port converter's output (line voltages). Avoid crossing two modulating reference signals to avoid the combination 4 dc-link short circuit.

Equal and variable frequency operation

A six-port converter can function in two

ways to overcome the restriction. 1) Equal frequency (EF) operation: as shown in Fig., V_{pv-abc} and $V_{dvr-xyz}$ must operate at the same frequency with minimal interphase. 7, a.

2) Both sets of outputs operate at varied frequencies. Without an output frequency restriction, this process is more versatile and may improve harmonic compensation [Fig. (7(b)). In contrast, complete modulation assumes t_c -max compensation time. The maximum DVR-VSI modulation index is m_i -max. $P_{dvr-vsi}$ is the active power needed to maintain nominal load voltage, and nt is transformer turns ratio. Further capacitor sizing details are supplied. Left and right ports cannot exceed unity. To avoid reference crossover, VF operation requires double the dc-link voltage (Fig.). 7(b). Here are more details on the six-port setup and EF/VF operations. PV/DVR-VSI per-phase depiction

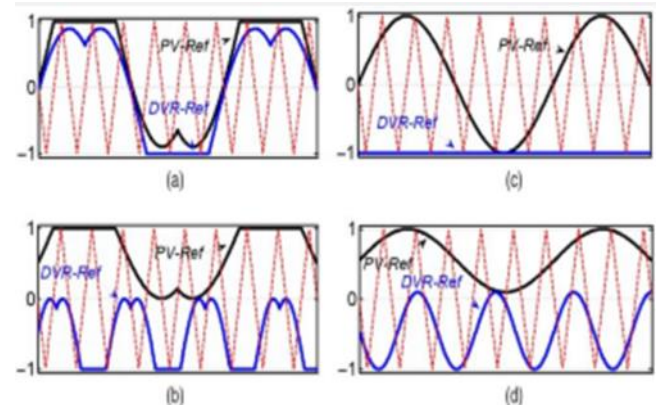


Fig.6: modulation references in healthy grid, VF, and sag modes..

In operation-1, PV-VSI injects active electricity into the grid while DVR-VSI is dormant. Fig. shows that the modulation index is PWM_{pv} and PWM_{dvr} , giving two sets of six gating signals: one for PV-VSI and zero for DVR-VSI. (6c). Despite a smaller modulation index, the PV-VSI injects active power during voltage sag (Mode-3) as the PCC voltage declines. Like

the illustration above, this helps the DVR-VSI reach the higher modulation index needed to correct for the sag. There is no crossover since increasing DVR-VSI invariably decreases PV-VSI reference. Thus, the suggested configuration avoids the reference crossover limitation. To perform the required procedure, generate nine gate pulses as described below. M_c represents the carrier signal amplitude in the two reference signals. These twelve gating signals can be sent directly to the PV and DVR VSIs using two independent six-switch inverters, as shown in Fig. 1. The middle row switches in the six-port converter are shared, therefore their gate pulses are produced by the logical OR operation of PWM signals for the left three DVR-VSI switches (Gdvr1–3) and the right three PV-VSI switches (Gpv4–6). Get the remaining nine gating signals, G_{n1-9} , this way:

4. OVERALL CONTROL SYSTEM

A single dc-link capacitor connects three H-bridge VSCs in the specified DVR converter. A single-phase transformer connects each VSC to the supply grid in series. The proposed FCI control system features three identical, independent controllers—one for each DVR single-phase VSC.

A phasor parameter estimator (digital filter) attenuates the measured signal's harmonics to estimate the phase FCI function's magnitudes and phase angles. Let the supply, load, and injected voltage fundamental frequency components be two identical least error squares (LES) filters. The DVR response is delayed by one cycle because the filter needs a full data window to attenuate all harmonics. Thus, disturbance attenuation and voltage

injection speed trade off. The planned LES filters use a 50-sample data window. Sampling at 10 kHz and estimating voltage phasor characteristics in 5 ms demonstrates that the LES filters attenuate voltage noise, harmonics, and distortions at frequencies above 200 Hz and below 50 Hz. This filter reduces distortion, harmonics, and noise in the sag compensation mode as well. The following section shows that this filter works well in FCI mode, even with arcing faults and significantly distorted voltage and current data.

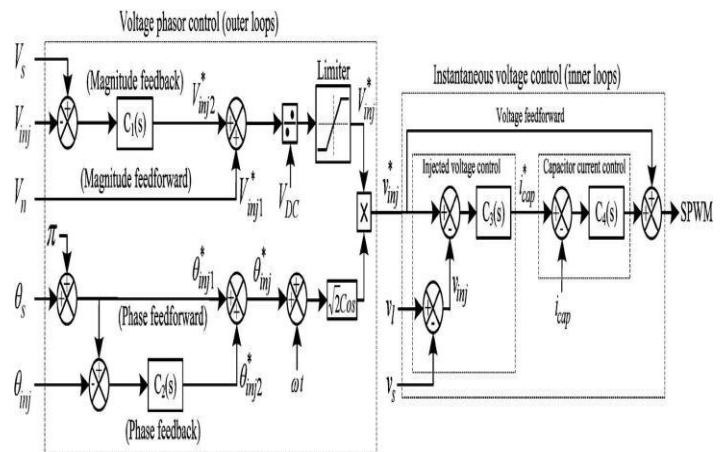


Fig.7 DVR Per-Phase Block Diagram.

Fig. shows the suggested DVR control system's per-phase block diagram for the FCI operation mode and nominal r.m.s. phase voltage. 7. The Fig. controlling system. 2 inputs harmonic filter capacitor current and dc-link voltage. This study uses overcurrent fault detection in its studies. The fault detection mechanism for each phase activates when the instantaneous current exceeds twice the rated load current.

The proposed multi-loop control system incorporates instantaneous voltage control and voltage phasor control loops. Damping harmonic filter transients with the inner loop improves the DVR's dynamic response and stability. FCI and sag compensation share an inner loop. When a downstream

fault is identified, the outer loop controls the injected voltage magnitude and phase load-side voltage to zero to interrupt the fault current and restore the PCC voltage. The next subsections cover the DVR's outer voltage phasor control and inner instantaneous voltage control for each phase.

Voltage Phasor Control System:

The required injected voltage phasor is the source voltage phasor in FCI operation mode, but in phase opposition. Perform voltage phasor control. Combining feed forward signals to the feedback control system and independently controlling voltage magnitude and phase improves transient response, speed, and steady-state error (Fig. 2). Two proportional-integral (PI) controllers (and) remove the steady-state errors of the injected voltage's phase and magnitude. The controller parameters are chosen to react quickly without steady-state inaccuracies. Polisetty Hema Sundar: Dynamic Voltage Regulator with Integrated Photovoltaic System Reduces Voltage Variations in Unreliability Situations Separate angles and a limiter filter magnitude (Fig. 2). Converting the phasor magnitude and phase angle yields the sinusoidal signal, the instantaneous voltage control reference signal.

Instantaneous Voltage-Control System:

In ideal conditions, the sinusoidal pulse width modulation (SPWM) unit can correct voltage sag directly from the phasor-based controller output. Under these conditions, harmonic filter resonance cannot be eliminated. To improve DVR stability and dynamic response, resonances are suppressed using an instantaneous injected voltage controller and a harmonic filter capacitor current controller.

By magnifying DVR filter resonance, a

large KV can reduce system stability. Thus, a feed forward loop increases DVR transient response and a moderate proportional gain controls voltage. Though limited by practical constraints like capacitor current noise amplification, measurement noise, and dc offset, a large dampens harmonic filter resonance more efficiently. The proportional gain is adjusted at its lowest value to dampen resonances. The PWM generator's signal is the current controller's output plus the feed-forward voltage.

Parameter	Value
Grid voltage (L-L) (rms) V_{base}	415 V
Line frequency	50 Hz
Nominal PV power (Base kVA)	10 kVA
Nominal load power	10 kVA
Nominal load power factor	0.8 lagging
DC link voltage	700 V
DC link capacitance	3000 μ F
Maximum shunt current, (I_{sh-max})	20 A
Series transformer rating/turn ratio	10 kVA/ 1:1
Filter inductor L_f and capacitance C_f	5 mH and 50 μ F
Grid impedance Z_{line}	0.5 + j0.05 Ω

Figure 7 shows simulation reference frame system settings.

5.SIMULATION STUDY

This section shows MATLAB/Simulink examination of the suggested system configuration's practicality. PV-VSI and DVR-VSI reference signals can be identified using their control blocks from the preceding section.

Three Phases Downstream Fault Interruption With DVR.:

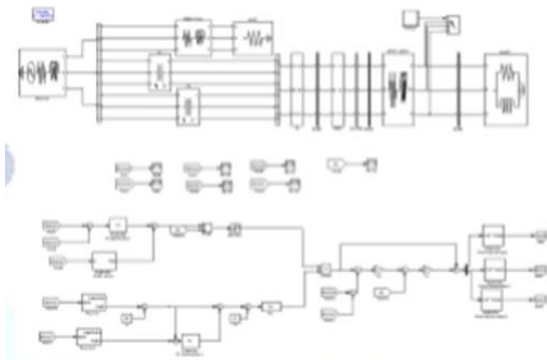


Fig.9:. Three-phase downstream fault interruption simulation block schematic with DVR.

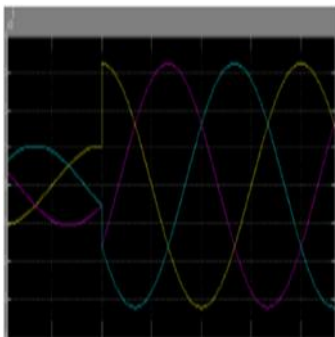


Fig.10 voltage on the y-axis and injected voltage with time on the x-axis.

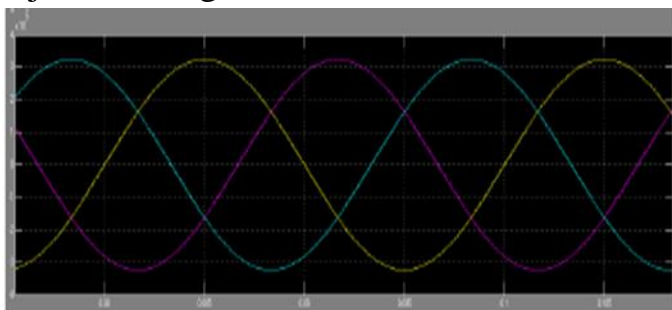


Fig.11:.. Show voltage on y and time on x.

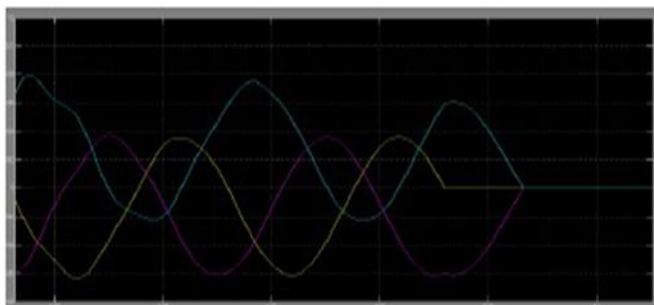


Fig.12: Current on y and time on x of a line current.

In fault and healthy grid modes Mode, sag mode, and no mode are PV generating modes for the interval based on active and

reactive power. Balanced three-phase and unbalanced operation might be difficult.

6.ANALYSIS OF STUDY:

The load can handle a modest voltage drop and phase angle jump. The loads' operation won't be affected by voltage magnitudes between 90% and 110% of the nominal voltage and 5% to 10% of the nominal state. This method's phase and magnitude control parameters can be achieved with a small energy infusion. Start with a basic overview of the high-level operation of one discrete filter type (see to preceding footnote). After providing this general picture, we will focus on the equations and how they are used in this filter. The filter employs feedback control to estimate a process by estimating its state at a particular moment and collecting (noisy) observations. Two types of filter equations exist: time update and measurement update. Time update equations project the current state and error covariance estimations forward to produce a priori estimates for the next time step. The measurement update equations improve the a posteriori estimate by adding a new measurement. Another way to think about time update equations is predictor equations.

7.CONCLUSION

This study introduces a new process for integrating a self-supported DVR with grid-connected PV. The proposed architecture completely demonstrates the PV and DVR method and expands the DVR's working range. DVR's resilience to severe grid disruptions is improved by using the PV plant's electric power. The described arrangement works in PV power generating and grid modes. The modes discussed include PV inactive, fault, sag, and healthy grid. Good simulated learning and experimental validation show that the

suggested setup works and can operate under unique settings. Modern load centers with strict voltage standards and on-web page PV iteration may benefit from the offered configuration.

REFERENCES

1. R. A. Walling, R. Saint, R. C. Dugan, J. Burke, and L. Kojovic, —Summary of distributed resources impact on power delivery systems,|| IEEE Trans. Power Del., vol. 23, no. 3, pp. 1636–1644, Jul. 2008.
 2. C. Meza, J. J. Negroni, D. Biel, and F. Guinjoan,—Energy-balance modeling and discrete control for single-phase grid-connected PV central inverters,|| IEEE Trans. Ind. Electron., vol. 55, no. 7, pp. 2734–2743, Jul. 2008.
 3. T. Shimizu, O. Hashimoto, and G. Kimura, —A novel high-performance utility-interactive photovoltaic inverter system,|| IEEE Trans. Power Electron., vol. 18, no. 2, pp. 704–711, Mar. 2003.
 4. S. B. Kjaer, J. K. Pedersen, and F. Blaabjerg, —A review of single-phase grid-connected inverters for photovoltaic modules,|| IEEE Trans. Ind. Appl., vol. 41, no. 5, pp. 1292–1306, Sep./Oct. 2005.
 5. T. Esram, J. W. Kimball, P. T. Krein, P. L. Chapman, and P. Midya,—Dynamic maximum power point tracking of photovoltaic arrays using ripple correlation control,|| IEEE Trans. Power Electron., vol. 21, no. 5, pp. 1282–1291, Sep. 2006.
 6. IEEE Recommended Practices and Requirements for Harmonic Control in Electrical Power Systems, IEEE Standard 519-1992, Apr. 1993, pp. 1–112.
 7. J. A. Martinez and J. M. Arnedo, —Voltage sag studies in distribution networks—Part I: System modeling,|| IEEE Trans. Power Del., vol. 21, no. 3, pp. 338–345, Jul. 2006.
 8. J. D. Li, S. S. Choi, and D. M. Vilathgamuwa,—Impact of voltage phase jump on loads and its mitigation,|| in Proc. 4th Int. Power Electron. Motion Control Conf., Xian, China, Aug. 14–16, 2004, vol. 3, pp. 1762–1766.
-